

# Journal of Geophysical Research: Oceans

## RESEARCH ARTICLE

10.1029/2018JC014302

**Key Points:**

- Annual Coccolithophore Bloom Index for the eastern Bering Sea shelf shows high interannual variability of bloom extent and distribution
- Coccolithophore Bloom Index is high during years with either very low or very high stratification
- Stratification strength influences coccolithophore bloom location (inner vs middle shelf)

**Correspondence to:**C. Ladd,  
carol.ladd@noaa.gov**Citation:**

Ladd, C., Eisner, L. B., Salo, S. A., Mordy, C. W., & Iglesias-Rodriguez, M. D. (2018). Spatial and temporal variability of coccolithophore blooms in the eastern Bering Sea. *Journal of Geophysical Research: Oceans*, 123, 9119–9136. <https://doi.org/10.1029/2018JC014302>

Received 22 JUN 2018

Accepted 10 NOV 2018

Accepted article online 14 NOV 2018

Published online 15 DEC 2018

## Spatial and Temporal Variability of Coccolithophore Blooms in the Eastern Bering Sea

C. Ladd<sup>1</sup> , L. B. Eisner<sup>2</sup>, S. A. Salo<sup>1</sup>, C. W. Mordy<sup>1,3</sup> , and M. D. Iglesias-Rodriguez<sup>4</sup>

<sup>1</sup>Pacific Marine Environmental Laboratory, NOAA, Seattle, WA, USA, <sup>2</sup>Alaska Fisheries Science Center, NOAA, Seattle, WA, USA, <sup>3</sup>Joint Institute for the Study of the Atmosphere and Ocean, University of Washington, Seattle, WA, USA, <sup>4</sup>Department of Ecology, Evolution, and Marine Biology, University of California, Santa Barbara, CA, USA

**Abstract** Coccolithophores are a widespread group of marine phytoplankton that produce plates of calcium carbonate that cover their cells. Large blooms of coccolithophores may significantly influence the biogeochemical properties of the ocean and atmosphere and trophic dynamics of the marine ecosystem. Because of the important implications of coccolithophore blooms, their timely monitoring and reporting is necessary for ecosystem management. To communicate with ecosystem management stakeholders, we developed an annual Coccolithophore Bloom Index (CBI) for the eastern Bering Sea shelf using satellite ocean color data. Comparisons between in situ and satellite data and the CBI (years 1997–2017) were used to examine the hypotheses regarding environmental influences on interannual bloom variability. A significant nonlinear relationship with summer stratification was found: the CBI was higher during years with either very low or very high stratification. In addition, while the blooms usually occurred over the middle shelf (50- to 100-m depth), more of the bloom was located over the shallow (30–50 m) inner shelf when stratification was low. Spatial correspondence between nutrient concentrations (nitrate and ammonium) and the areal extent of the coccolithophore bloom provides tantalizing but nonconclusive evidence that nutrient availability plays a role in bloom formation and location.

**Plain Language Summary** Intense blooms of coccolithophores, phytoplankton that occur in all of the world's oceans, have been implicated in seabird die-offs and other effects on the food web. These blooms turn the ocean milky white and can be seen from space. Because of important implications of coccolithophore blooms, monitoring and reporting is necessary for ecosystem management. We developed a measure of spatial extent of coccolithophore blooms in the Bering Sea each September using satellite ocean color data and examined what conditions are favorable to bloom formation. The water column in this region is typically two layered during summer with warmer surface layer separated from colder deep layer. We found that the difference between the two layers (strength of stratification) was important. Coccolithophore blooms were larger during years with either very weak or very strong stratification. In addition, while blooms usually occurred over the middle shelf (50- to 100-m depth), more of the bloom was located over the shallow (30–50 m) inner shelf when stratification was weak. Nutrient availability likely plays a role in bloom formation and location. Understanding the factors leading to coccolithophore blooms may allow us to forecast blooms in the future, providing important advance information for resource managers.

### 1. Introduction

Coccolithophores are a widespread group of marine phytoplankton that produce plates of calcium carbonate (coccoliths) that cover their cells. Large blooms of coccolithophores may significantly influence the biogeochemical properties of the ocean and atmosphere through formation of calcium carbonate, organic carbon, and dimethyl sulfide (e.g., Holligan et al., 1993; Raitsos et al., 2006). Feedbacks between anthropogenic increases in atmospheric CO<sub>2</sub> and coccolithophore productivity, and calcium carbonate production and export to the benthos have important biogeochemical implications (e.g., Delille et al., 2005; Iglesias-Rodriguez et al., 2008; Riebesell et al., 2000; Zondervan et al., 2001).

In addition to their biogeochemical impacts, coccolithophore blooms also have an effect on the trophic dynamics of the ecosystem. For example, because of their small size, coccolithophores contribute to a longer, less efficient food chain than larger phytoplankton, potentially resulting in less transfer of energy to upper trophic levels (Hunt et al., 1999; Olson & Strom, 2002). Also, coccolithophore blooms dramatically alter the

optical properties (reduce transparency) of the water column and have been associated with seabird die-offs and changing distributions of fish and other upper trophic level consumers (Vance et al., 1998).

Sediment records indicate that populations of the coccolithophorid *Emiliania huxleyi* have been present in the southeastern Bering Sea since the late 1970s (Harada et al., 2012). An increase of *E. huxleyi* in the sediment record was related to a climate regime shift that occurred in 1976–1977 and was related to enhanced stratification due to increasing sea surface temperature and decreasing surface salinity. While Harada et al. (2012) found that *E. huxleyi* have been present in the Bering Sea since the 1970s, Merico et al. (2003) found no evidence of coccolithophore blooms using Coastal Zone Color Scanner or Advanced Very High Resolution Radiometer satellite data from 1978 through 1995. Advanced Very High Resolution Radiometer data suggest a small bloom in summer 1996 (prior to a massive bloom in 1997), suggesting that cell densities required for satellite identification of coccolithophore blooms did not occur until 1996 (Merico et al., 2003).

A large coccolithophore bloom (primarily *E. huxleyi*) occurred in 1997 (Napp & Hunt, 2001; Stockwell et al., 2001; Vance et al., 1998) and for several years thereafter. The 1997 bloom was associated with a die-off of short-tailed shearwaters (*Puffinus tenuirostris*), a seabird commonly seen in these waters (Baduini et al., 2001). It has been argued that the bloom may have made it difficult for the shearwaters to see their zooplankton prey from the air (Lovvorn et al., 2001) and thus limited their access to food. Since 1997, coccolithophore blooms in the eastern Bering Sea have become common, although high interannual variability is observed. Over the last few decades, diatom abundance has increased, but increases in the production rate of *E. huxleyi* exceeds that of diatoms (Harada et al., 2012). Satellite ocean color data suggest that blooms are only found where water depths are between 20 and 100 m, typically occur in years with strong stratification, and usually peak in September (Iida et al., 2012).

Merico et al. (2004) used a time-dependent ecosystem model combined with field and satellite data to examine phytoplankton succession in the southeastern Bering Sea shelf. They found that the shallow mixed layer depth, high sea surface temperature, and high photosynthetically active radiation (PAR) of 1997 played an important role in promoting the development of the coccolithophore bloom that year (Merico et al., 2004). They also found that selective grazing of diatoms by microzooplankton was responsible for the extended length of the coccolithophore bloom (3–4 months), a result also supported by dilution experiments performed during the 1999 *E. huxleyi* bloom (Olson & Strom, 2002). Merico et al. (2004) suggest that the unusual conditions of 1997 allowed a seed population in the Bering Sea that resulted in blooms in subsequent years (1998–2000), fading away by 2001 as climate returned to less anomalous conditions.

While various mortality processes are undeniably important (e.g., Irigoien et al., 2005), physical mixing and nutrient supply have been proposed to be primary processes controlling seasonal dynamics of phytoplankton succession (Margalef, 1978). For example, diatoms thrive under enhanced nutrient availability, whereas coccolithophores and dinoflagellates are superior competitors under stratified conditions that limit nutrient supply (Cermeno et al., 2008; Falkowski & Oliver, 2007; Iglesias-Rodriguez et al., 2002; Margalef, 1997). Using satellite data, Hopkins et al. (2015) found not only evidence to support the canonical view of succession of phytoplankton in some regions (particularly shelf environments) but also strong evidence of coexistence of phytoplankton populations in other regions (particularly in open ocean environments).

Oceanographic sampling has historically focused on nitrate, nitrite, phosphate, and silicate (required by diatoms). However, nitrate is not the sole source of nitrogen and *E. huxleyi* prefers ammonium to nitrate (Page et al., 1999; Song & Ward, 2007). Moreover, the largest proportion of the dissolved nitrogen is organic (Antia et al., 1991) and coccolithophores can use nanomolar concentrations of dissolved organic nutrients including dissolved organic phosphate. For example, *E. huxleyi* has highly efficient alkaline phosphatase and other enzymes to hydrolyze and acquire dissolved organic phosphate as well as diverse nitrogen acquisition enzymes including organic nitrogen and many ammonium transporters (Read et al., 2013; Riegman et al., 2000). Although high N:P ratios have been considered an important factor for the success of *E. huxleyi* (Riegman et al., 2000; Tyrrell & Taylor, 1996), model results suggested that the N:P ratio did not play a role in the Bering Sea blooms (Merico et al., 2004).

Because of the important biogeochemical and ecosystem implications of coccolithophore blooms, their timely monitoring and reporting is necessary for ecosystem management. Fortunately, satellite ocean color data allow timely characterization of blooms spatially and temporally. To communicate with ecosystem management stakeholders, we have developed a Coccolithophore Bloom Index (CBI) that was originally

published in the 2016 Eastern Bering Sea Ecosystem Considerations report (Ladd et al., 2016). The intent is that this index will be updated annually in early October and included in future iterations of the report.

Using in situ and satellite data from the eastern Bering Sea shelf in comparison with the new CBI, we examine hypotheses regarding bottom-up influences (stratification, light, and nutrient availability) on interannual coccolithophore bloom variability. We also describe spatial (horizontal coverage and vertical water column) variations in the coccolithophore blooms in relation to environmental factors for three recent bloom years (2009, 2011, and 2014). While spatial availability of in situ data is quite variable from year to year, these 3 years have relatively broad spatial coverage over the eastern Bering Sea shelf during August/September.

### 1.1. Physical Setting

The eastern Bering Sea is home to a rich and productive ecosystem with very valuable resources. The Bering Sea pollock (*Gadus chalcogrammus*) fishery is the largest in the United States by volume and among the largest fisheries in the world (Haynie & Huntington, 2016). Prior to 2000, the southeastern shelf of the Bering Sea was characterized by high interannual variability in sea-ice extent and temperature. After 2000, the variability shifted to longer periods with stanzas of warm or cold conditions lasting of the order of 5 years. While these stanzas have been defined in terms of temperature and sea-ice extent, many variables are associated with the warm or cold conditions including current direction, types and abundances of phytoplankton and zooplankton, year-class strength of pollock and Pacific cod, and the distribution and relative abundance of fin whales (Eisner et al., 2016; Stabeno, Kachel et al., 2012).

The eastern Bering Sea shelf comprises three domains (inner, middle, and outer) with distinct hydrographic characteristics during the summer (Coachman & Charnell, 1979; Kinder & Schumacher, 1981; Schumacher & Stabeno, 1998). The inner domain (depth  $< 50$  m) is typically well mixed and nutrient poor throughout the summer, except downstream of Bering Canyon where there is a strong nutrient flux from the slope (Mordy et al., 2017). The middle domain ( $50 \text{ m} < \text{depth} < 100 \text{ m}$ ) is characterized by a strong two-layer system in summer with the surface wind-mixed layer separated from a deep tidally mixed layer by a sharp thermocline. After the spring phytoplankton bloom, the surface mixed layer of the middle domain is typically nutrient depleted although occasional summer mixing events can mix nutrients from the deep layer into the surface layer (Sambrotto et al., 1986; Whitledge et al., 1986). The outer domain ( $100 \text{ m} < \text{depth} < 180 \text{ m}$ ) is characterized by mixed upper and lower layers separated by gradually increasing density. The three domains are separated by fronts or transition zones. The inner front separates the inner and middle domains and approximately coincides with the 50-m isobath (Kachel et al., 2002). The middle front separates the middle and outer domains, and the shelf break front separates the outer shelf from the basin (Favorite et al., 1976; Kinder & Coachman, 1978; Kinder & Schumacher, 1981). During summer, mixing at the inner front can mix water from the bottom layer of the middle shelf, introducing nutrients and colder water into the surface mixed layer (Kachel et al., 2002; Mordy et al., 2017; Stockwell et al., 2001).

In addition to the three cross-shelf domains, the eastern Bering Sea shelf is also divided at  $\sim 60^\circ\text{N}$  between a northern domain and a southern domain (Stabeno, Farley et al., 2012). The northern middle shelf domain is characterized by a low-salinity surface lens, cold bottom temperatures, a thick pycnocline, and subsurface chlorophyll maxima. The southern shelf is characterized by a thin pycnocline ( $< 3 \text{ m}$ ) determined largely by temperature alone. Subsurface chlorophyll maxima are uncommon on the southern middle shelf (Stabeno, Farley et al., 2012).

## 2. Methods

### 2.1. Coccolithophore Bloom Index

#### 2.1.1. SeaWiFS and MODIS

Sea-viewing Wide Field-of-view Sensor (SeaWiFS; National Aeronautics and Space Administration [NASA] Goddard Space Flight Center, 2014 Reprocessing-b) and Moderate Resolution Imaging Spectroradiometer (MODIS) Aqua (NASA Goddard Space Flight Center, 2014 Reprocessing-a) Level 1 data files for satellite passes over the Bering Sea were obtained from the Ocean Color website (<http://oceancolor.gsfc.nasa.gov>) and processed using SeaDAS, a set of ocean color programs available from <http://seadas.gsfc.nasa.gov/>, to create data files with 1-km resolution.

**Table 1**  
Coccolithophore Bloom Index (CBI)

Year	Satellite	Middle shelf	Inner shelf	Total
1997 (C)	SeaWiFS	<b>130,391</b>	<b>36,141</b>	<b>166,532</b>
1998 (W)	SeaWiFS	<b>58,776</b>	<b>18,983</b>	<b>77,759</b>
1999 (C)	SeaWiFS	<b>99,791</b>	<b>30,344</b>	<b>130,134</b>
<b>2000 (A)</b>	<b>SeaWiFS</b>	<b>68,306</b>	<b>37,566</b>	<b>105,873</b>
2001 (W)	SeaWiFS	14,835	6,209	21,044
2002 (W)	MODIS	10,132	1,897	12,029
2003 (W)	MODIS	18,815	1,611	20,426
2004 (W)	MODIS	39,163	4,914	44,077
2005 (W)	MODIS	12,162	3,792	15,954
2006 (A)	MODIS	34,191	373	34,564
<b>2007 (C)</b>	<b>MODIS</b>	<b>66,101</b>	<b>10,326</b>	<b>76,427</b>
2008 (C)	MODIS	3,579	862	4,441
<b>2009 (C)</b>	<b>MODIS</b>	<b>72,576</b>	<b>3,279</b>	<b>75,855</b>
2010 (C)	MODIS	4,608	2,109	6,717
<b>2011 (C)</b>	<b>MODIS</b>	<b>70,772</b>	<b>41,802</b>	<b>112,574</b>
2012 (C)	MODIS	273	3,656	3,930
2013 (C)	MODIS	14,637	2,429	17,066
<b>2014 (W)</b>	<b>MODIS</b>	<b>60,658</b>	<b>22,268</b>	<b>82,927</b>
2015 (W)	MODIS	32,302	2,893	35,195
<b>2016 (W)</b>	<b>MODIS</b>	<b>58,797</b>	<b>8,767</b>	<b>67,563</b>
2017 (A)	MODIS	9	431	440
<b>Mean</b>		<b>41,470</b>	<b>11,460</b>	<b>52,930</b>
<b>Standard deviation</b>		<b>35,753</b>	<b>13,774</b>	<b>47,332</b>

Note. Area ( $\text{km}^2$ ) covered by coccolithophore blooms in September of each year over the middle shelf (50- to 100-m depth) and inner shelf (30- to 50-m depth). W/C/A designation of each year refers to warm, cold, or average conditions as defined by Stabeno et al. (2017; 2012). Nine above average (bloom) years are noted in bold. MODIS = Moderate Resolution Imaging Spectroradiometer; SeaWiFS = Sea-viewing Wide Field-of-view Sensor.

Frequent, extensive cloud cover over the Bering Sea results in missing ocean color data, which was more pronounced in August than in September. Thus, in calculating our CBI, we restricted our attention to the month of September that also corresponds to the period when coccolithophore blooms typically peak (Iida et al., 2012).

### 2.1.2. Coccolithophore Bloom Index

The high reflectance and unique spectral signature of coccolithophore blooms allow for their identification from space. The algorithm for detecting coccolithophores from satellite ocean color data was initially developed using Coastal Zone Color Scanner imagery (Brown, 1995; Brown & Yoder, 1994). Normalized water-leaving radiance ( $nL_w$ ) at various wavelengths and ratios were selected for the algorithm based on separating the spectral signatures of various conditions (coccolithophore blooms, clear blue water, sediment-laden water, etc.). When the first SeaWiFS-observed coccolithophore bloom was detected in the Bering Sea in late summer of 1997 (Vance et al., 1998), the algorithm did not adequately identify the bloom. After subsequent coccolithophore blooms in the North Atlantic and the Bering Sea in 1998, the algorithm was revised (Robinson, 2000) and adopted by the U.S. NASA.

Using a combination of satellite and ship-based optical observations, Iida et al. (2002) found that in situ measurements of  $nL_w$  yielded values that differed from the standard NASA coccolithophore values. Electron microscopy from their cruises in 1998 and 2000 confirmed that the blooms were composed of *E. huxleyi* (Iida et al., 2002). High concentrations of colored dissolved organic matter and detritus on the Bering Sea shelf result in high light absorption at short wavelengths in the surface waters (Sasaki et al., 2001). Thus, light absorption at 443 nm is higher and  $nL_w$  is lower than in other regions. Low values of  $nL_w$  (443 nm) result in ratios  $nL_w$  (443/555) and  $nL_w$  (443/510) that are lower than the standard NASA coccolithophore mask. Thus, Iida et al. (2002) defined new threshold

values to determine coccolithophore bloom conditions and applied that methodology to evaluate coccolithophore blooms in the Bering Sea from SeaWiFS and MODIS data from 1997 through 2008 (Iida et al., 2012). While there is a wavelength channel difference between SeaWiFS (510 nm) and MODIS (531 nm), Iida et al. (2012) recommend simply replacing the SeaWiFS 510-nm channel with the MODIS 531-nm channel in defining the coccolithophore mask (see below).

We use Iida's methods (Iida et al., 2012, 2002) to create an index of coccolithophore area in square kilometer (Table 1). Using only pixels that are cloud free and at zenith angles less than 55°, the following criteria were used to create a coccolithophore mask:

$$nL_w(443 \text{ nm}) > 1.1 \text{ mW} \cdot \text{cm}^{-2} \cdot \mu\text{m}^{-1} \cdot \text{sr}^{-1}$$

$$nL_w(555 \text{ nm}) > 0.8 \text{ mW} \cdot \text{cm}^{-2} \cdot \mu\text{m}^{-1} \cdot \text{sr}^{-1}$$

ratios :

$$0.64 < nL_w(443/555 \text{ nm}) < 1.55$$

$$0.7 < nL_w(443/510 \text{ nm}) < 1.0 \text{ (SeaWiFS); } 0.7 < nL_w(443/531 \text{ nm}) < 1.0 \text{ (MODIS)}$$

$$0.91 < nL_w(510/555 \text{ nm}) < 1.6 \text{ (SeaWiFS); } 0.91 < nL_w(531/555 \text{ nm}) < 1.6 \text{ (MODIS)}$$

To calculate the area of the bloom, we included each pixel that satisfies the coccolithophore mask criteria for at least 50% of the time that it is cloud free during the month of September. The CBI is defined as the total area of the bloom in the region south of 60°N and deeper than 30-m depth (Figure 1), calculated by summing the area ( $\text{km}^2$ ) represented by these pixels.

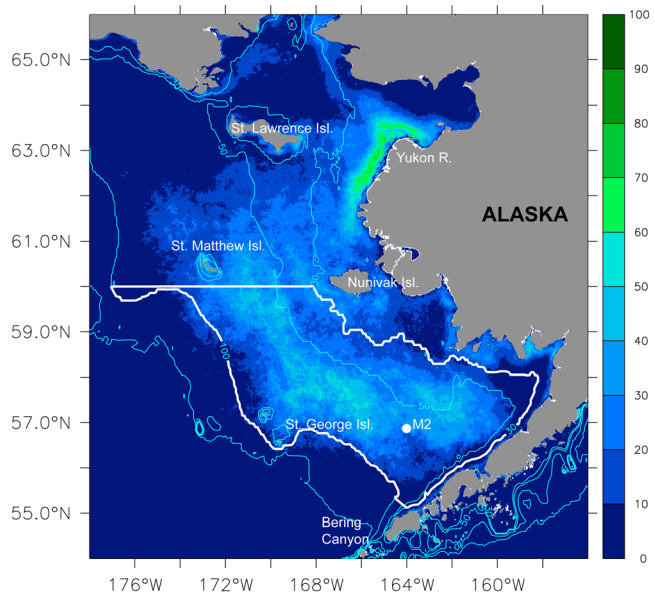


**Figure 1.** Average (over years 1997–2016) of spatial CBI. Color indicates the percent of cloud-free days in September for which each satellite ocean color pixel indicates coccolithophores. White contour indicates the region used in calculating the CBI. Bathymetric contours (30, 50, 100, and 200 m) are shown in light blue. Location of mooring M2 is indicated by white dot. CBI = Coccolithophore Bloom Index.

The CBI was limited to this region to avoid highly reflective waters in shallow waters near the coast and around St. Matthew and St. Lawrence Islands that can result from resuspended diatom frustules rather than coccolithophores (Broerse et al., 2003), and to avoid sediments associated with the Yukon River. Hence, our attention was restricted to the region south of the transition noted in the introduction. Because blooms are often largely confined to either the middle shelf or the inner shelf, two indices were calculated, one for the middle shelf (50- to 100-m depth) and one for the inner shelf (30- to 50-m depth).

SeaWiFS data are available beginning in September 1997; MODIS data began in 2002. We examined differences between the CBI calculated from SeaWiFS and that calculated from MODIS for 2002–2004, and found that the SeaWiFS index was notably higher than the MODIS index (averaging 16% higher for the middle shelf and 37% for the inner shelf). Thus, the CBI for 1997–2001 (calculated from SeaWiFS data) includes a reduction of 16% for the middle shelf and 37% for the inner shelf to account for the bias. The CBI for 2002–2016 was calculated from MODIS data with no bias correction.

## 2.2. In Situ Data

In situ data from the eastern Bering Sea shelf collected via shipboard measurements and moorings were used to examine relationships between coccolithophore blooms and the physical environment.

### 2.2.1. Shipboard Data

Bering-Arctic-Subarctic Integrated Survey (BASIS) hydrographic data have been collected since 2002 at stations spaced ~60 km apart, over a nominal survey grid spanning the shelf (160–172°W, 54.5–65°N). The stations actually sampled in each year can vary considerably with better coverage in some years than others. Sampling typically occurs from mid-August to early October, although survey start and end times can vary by up to 3 weeks among years. In addition, a transect along the 70-m isobath of the eastern Bering Sea shelf was typically sampled in September each year. Data from 2009, 2011, and 2014 from both the BASIS grid and the 70-m isobath transect are discussed in section 3.

Shipboard data include vertical profiles of conductivity-temperature-depth (CTD), chlorophyll *a* (Chl *a*) fluorescence and percent light transmission. These profiles were collected from surface to 5–10 m off bottom with a 911 plus Sea Bird Electronics CTD equipped with a Wetlabs Wet-Star or ECO FLNTU fluorometer and a C-Star transmissometer. CTD data were processed with standard Sea Bird Electronics algorithms and binned into 1-m averages.

In addition, discrete water samples were collected from Niskin bottles for nutrients and Chl *a* at 2 to 6 depths distributed above and below the pycnocline. Nutrient samples were filtered with 0.45 cellulose acetate syringe filters to remove particulates (except for 2009 samples) and frozen for later analysis of dissolved phosphate, silicic acid, nitrate, nitrite, and ammonium at a shore-based facility using colorimetric methods (Gordon et al., 1994; Joint Global Ocean Flux Study, 1994). Chl *a* samples were filtered through Whatman glass fiber filters (GF/F, nominal pore size 0.7  $\mu$ m) to estimate total Chl *a*. Filters were frozen at –80 °C and analyzed within 6 months with a Turner Designs (TD-700) benchtop fluorometer following standard methods (Parsons et al., 1984). The in vivo fluorescence (CTD) data were calibrated with discrete Chl *a* samples (Eisner et al., 2016).

### 2.2.2. Moorings

Mooring M2 (56.9°N; 164.1°W) in the southeast middle shelf domain of the Bering Sea has been collecting data almost continuously since 1995 (Stabeno et al., 2010). Due to weak advection in this region, M2 is largely representative of the entire southeastern middle shelf (Stabeno et al., 2001). The shallowest instruments during autumn are deployed at ~11 m with temperature measured approximately every 3 m in the upper 30 m and every 5–7 m below 30 m (Stabeno, Kachel et al., 2012). To account for differing instrument depths on the mooring during different deployments, temperature data were linearly interpolated to 1-m spacing.

The strong two-layer system of the middle shelf during summer is primarily determined by temperature differences (Ladd & Stabeno, 2012; Stabeno, Farley et al., 2012) allowing estimation of stratification simply as the temperature difference between the surface mixed layer (12 m) and the bottom mixed layer (50 m). To compare late summer stratification with the CBI, we average this temperature difference over the month of August each year. Maximum stratification occurs during August, and monthly-average August stratification has been shown to be a good index of the interannual variability of summer stratification in the southeast Bering Sea shelf (Ladd & Stabeno, 2012). August stratification represents initial conditions near the beginning of the September bloom period.

### 3. Results

#### 3.1. Interannual Variability

An average (over years: 1997–2016) of September coccolithophore tagged pixels illustrates locations where coccolithophores were most commonly observed (Figure 1). As expected, high values were observed very close to the coast and in the shallow waters around St. Matthew and St. Lawrence Islands. In addition, very high values were observed along the coast between  $\sim 60^{\circ}\text{N}$  and  $64^{\circ}\text{N}$  likely associated with the Yukon River plume. As noted previously, high values in these regions are likely due to highly reflective resuspended sediment, not coccolithophores (i.e., Broerse et al., 2003), and were therefore excluded from the CBI calculation by restricting the index to regions south of  $60^{\circ}\text{N}$  and deeper than 30 m. Clearly, September coccolithophore blooms were most frequent in the highly stratified middle shelf region although significant bloom activity (averaging 22% of total bloom area) was observed on the inner shelf, particularly south of  $\sim 58^{\circ}\text{N}$ . Ocean color data from the outer shelf and basin (water depth  $> 100$  m) exhibited almost no evidence of coccolithophore blooms.

Over the 21-year satellite time series, the CBI averaged almost  $53,000\text{ km}^2$  and exhibited high interannual variability (Figures 2 and 3, and Table 1). The time series began in September 1997 with the largest coccolithophore bloom ever observed in the Bering Sea (over  $166,000\text{ km}^2$ ). This bloom was associated with very strong stratification that summer along with other anomalous environmental conditions (Merico et al., 2004; Napp & Hunt, 2001; Stockwell et al., 2001). Large blooms continued each September for the next 3 years. In 2001, while small regions of bright water associated with coccolithophores were still observed (Figure 2), the bloom area was much smaller. The bloom area averaged over  $120,000\text{ km}^2$  over the 4 years 1997–2000, while the bloom in 2001 was  $\sim 17\%$  of that at  $21,044\text{ km}^2$  (Figure 3 and Table 1). The annual bloom area remained below average for 6 years until 2007 (another year with very strong stratification), when an above average bloom area ( $> 76,000\text{ km}^2$ ) initiated a series of alternating high/low years.

While, on average, coccolithophores were most frequently observed in the middle domain, the proportion in the middle versus the inner domains varies substantially from year to year. The very large blooms in 1997–1999 covered a significant portion of the shelf (both inner and middle domains), and the fraction of the bloom in the inner domain was about average (22–24%) in all three years. In 2000, the proportion of the bloom in the inner domain increased to 35% and parts of the middle domain were coccolithophore free (Figure 2). Over the nine above average years in the CBI, the percent of bloom pixels in the inner domain varied from 4% (2009) to 37% (2011). In some years, the distribution of coccolithophores appears to be associated with the inner front (i.e., 2004 and 2014) along the 50-m isobath (Figure 2).

Many investigations have suggested a relationship between stratification and coccolithophore blooms, with strong stratification providing favorable conditions for blooms (e.g., Harada et al., 2012; Iida et al., 2012). The occurrence of blooms on the inner shelf ( $< 50\text{-m}$  depth) suggests that strong stratification is not a necessary condition, as the inner shelf is typically well mixed throughout the year. Comparisons between August temperature stratification in the middle shelf region and the CBI suggest a significant nonlinear relationship ( $p$  value = 0.003;  $R^2 = 0.40$ ; Figure 4). As expected, the unprecedented 1997 bloom occurred during the year with the strongest stratification (2007 had similar strong stratification). If 1997 is removed from the analysis, the correlation is weaker ( $p$  value = 0.02;  $R^2 = 0.33$ ) but still significant. Interestingly, most of the years with the weakest stratification (1998, 1999, 2000, and 2011, but not 2001) also exhibited large blooms. The final year of data included in this study (2017) was notable as it exhibited the lowest CBI of the entire satellite record (Figures 2–4 and Table 1) and was a relatively high year in terms of stratification.

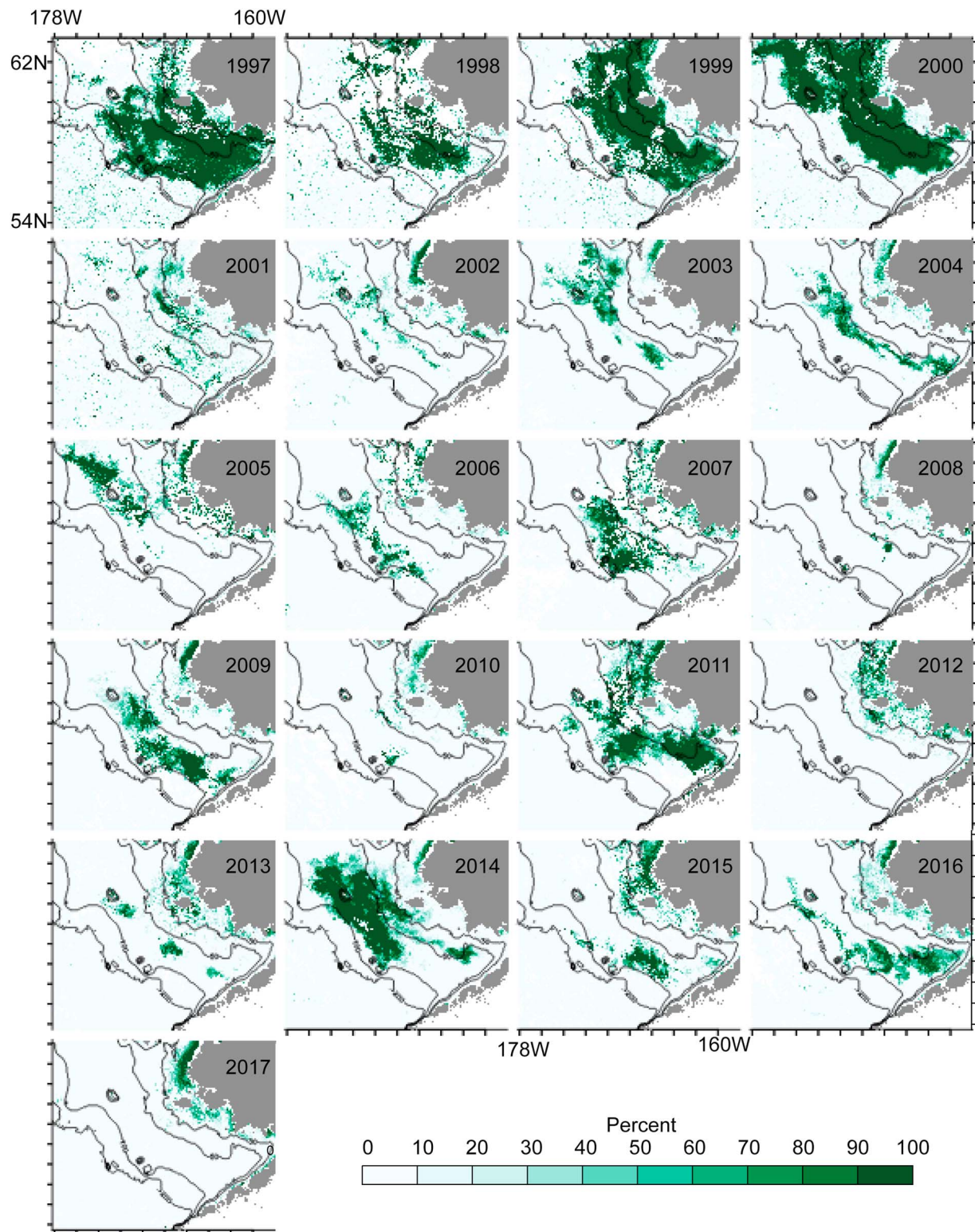


**Figure 2.** Spatial CBI. Percent of cloud-free days in September for which each satellite ocean color pixel indicates coccolithophores. CBI = Coccolithophore Bloom Index.

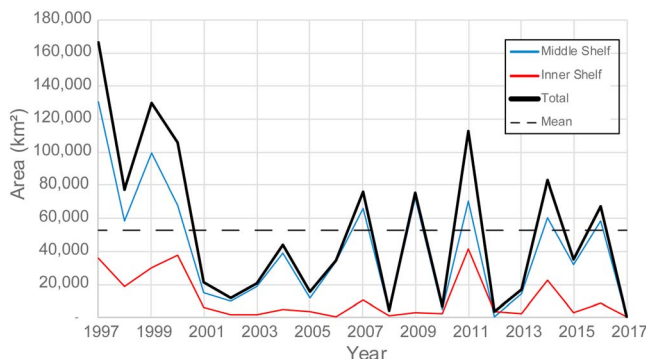


**Figure 3.** Coccolithophore Bloom Index (CBI). Area ( $\text{km}^2$ ) covered by coccolithophore bloom in September over the middle shelf (blue), inner shelf (red), and total (thick black). Dashed line indicates 20-year mean.

CBI = Coccolithophore Bloom Index.

If we examine only the 9 years with above average CBI, four of those years have very weak stratification (1998, 1999, 2000, and 2011), four have above average stratification (1997, 2007, 2009, and 2014), and one has average stratification (2016). The percent of the bloom area that occurred in the inner domain was significantly different ( $p$  value = 0.05) in low and high stratification years, averaging 30% for the low stratification years and 17% for the high stratification years. Composite maps showing the spatial distribution of the blooms in the high stratification years compared with the low stratification years (Figure 5) exhibit a bloom that is mainly restricted to the middle shelf during high stratification years. During the low stratification years, the bloom was much more extensive in the inner shelf region and farther north (although the region north of 60°N does not contribute to the index).

Interestingly, while the temperature regime and sea-ice extent of the eastern Bering Sea influences many variables from zooplankton to whales (Stabeno, Kachel et al., 2012), it does not appear to play a role in the

observed interannual variability of stratification on the southeast shelf (Ladd & Stabeno, 2012) or on the CBI (Table 1). Both extensive ice cover and cold temperatures (i.e., 1999 and 2007) and contracted ice cover and warm temperatures (i.e., 2014 and 2016) can precede extensive blooms in September.

Light irradiance has also been suggested to be important to coccolithophore blooms, at least in the case of *E. huxleyi*, as they are remarkably resistant to photoinhibition even without coccoliths (Houde et al., 2005) and thus have tolerance for high light intensity (Nanninga & Tyrrell, 1996). Unfortunately, in situ PAR data are limited. Thus, we examined various proxies for light availability in the region, including satellite PAR measurements and incoming shortwave radiation from the National Center for Environmental Prediction Reanalysis (Kalnay et al., 1996) and from the M2 mooring over various locations and regional averages. Light availability to phytoplankton can be a function of light attenuation in the water column and mixed layer depth. However, summer mixed layer depths in the region are not very variable (< 10 m) and our region is away from land where sediment load can influence light attenuation. Thus, we expect that the water column light environment is primarily a function of PAR at the initiation of the bloom. Note that the bloom itself can have significant influence on light attenuation (see next section). Nevertheless, we examined relationships with mixed

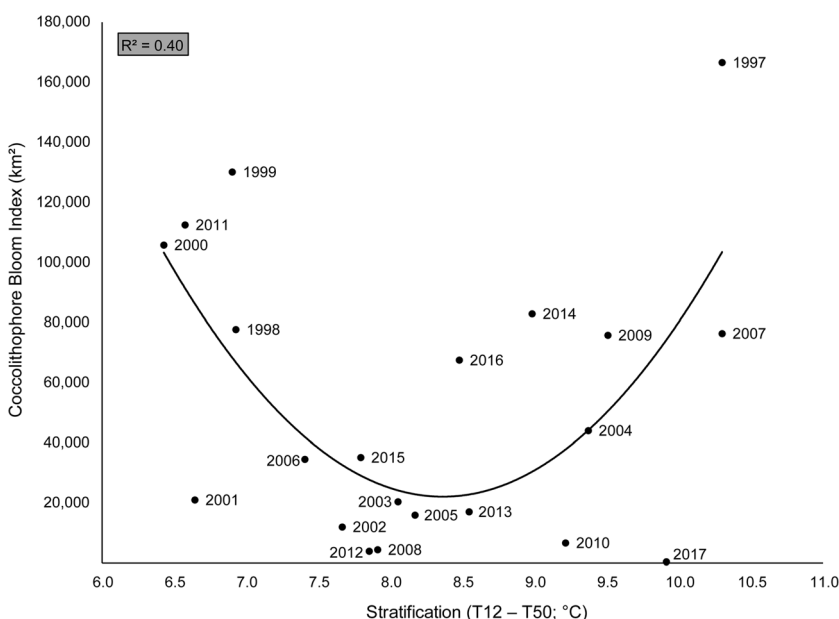


**Figure 4.** Scatterplot of total CBI ( $\text{km}^2$ ) versus temperature stratification ( $T_{12} - T_{50}$ ; °C) at M2. Second-order polynomial fit (line) is significant ( $p$  value < 0.003). CBI = Coccolithophore Bloom Index.

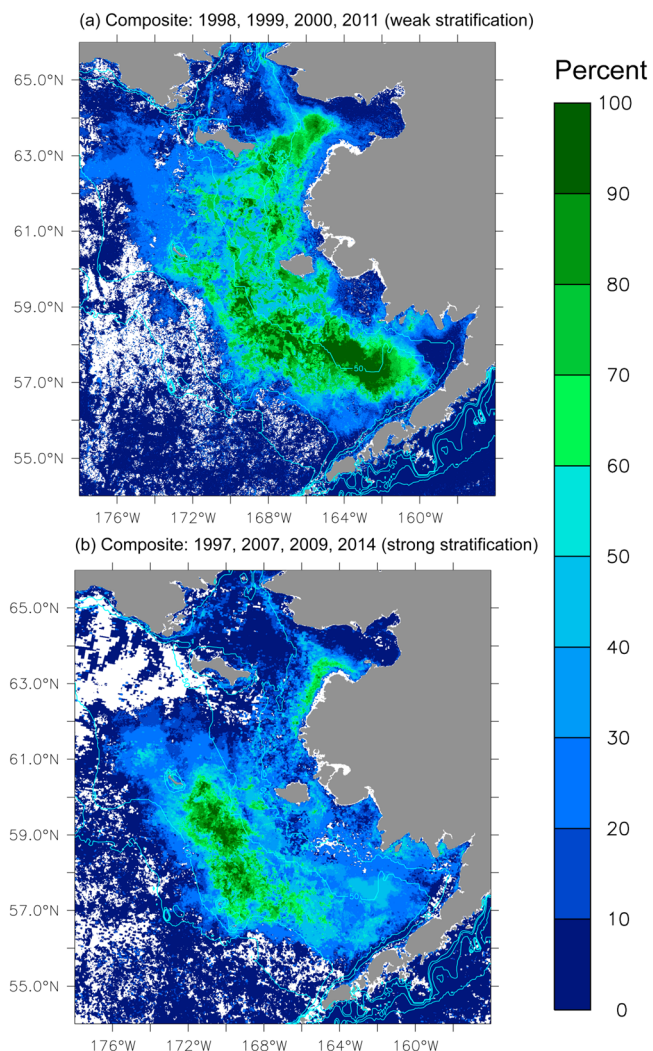


**Figure 5.** Composites of years with above average CBI and (a) weak stratification (1998, 1999, 2000, and 2011) and (b) strong stratification (1997, 2007, 2009, and 2014). CBI = Coccolithophore Bloom Index.

observed throughout the water column with lower percent light transmission in bloom than nonbloom waters at surface and at depth, as observed in 2014, likely due to at least partially actively growing cells in surface waters and the settling of cells and coccoliths below the pycnocline.

### 3.2.2. Stratification

Both 2009 and 2014 exhibited above average stratification (Figure 4) as measured at M2 (Figure 1), and the coccolithophore blooms were confined mostly to the middle shelf while 2011 exhibited weaker stratification with more of the bloom over the inner shelf (Figure 2 and Table 1). While vertical temperature difference can be used as a proxy for stratification on the southern middle shelf, salinity can play a role in the inner and outer shelf regimes and over the northern part of the shelf (Ladd & Stabeno, 2012; Stabeno, Farley et al., 2012). Thus, to examine spatial variability of stratification using cruise data, we used the difference between  $\sigma_0$  at depth (shallower of 50 m or the bottom depth) and  $\sigma_0$  at 12 m (Figure 7). Because the timing of the cruises in each year varies, and the seasonal cycle of stratification is strong (Ladd & Stabeno, 2012), interannual comparison of stratification from cruise CTD data does not allow for a meaningful comparison. To examine spatial variability within each year, we show the anomaly in stratification from that year's average over all stations (Figure 7).

In 2009, the strongest stratification was observed in the northern middle shelf in a region with little bloom signature. South of 60°N, stratification along the middle shelf coincident with the bloom was near the

layer depth as well. However, an examination of the CBI and the light environment (using these various proxies) and mixed layer depth shows no significant correlations (not shown).

### 3.2. Spatial Variability: 2009, 2011, and 2014

In an attempt to understand conditions favorable to coccolithophore bloom formation, we examined case studies of selected years. Unfortunately, variations in data availability in each year considerably limited this analysis. Thus, we restrict our examination to a few recent bloom years with high data availability. Recent years with strong coccolithophore blooms but differing stratification environments include 2011 (very weak stratification) and 2009 and 2014 (strong stratification, Figure 4). We examined the physical and chemical environment and associated spatial distribution of the blooms in these years in more detail.

In the previous section (3.1 Interannual Variability), we used a temporally consistent time series from mooring data to examine interannual relationships between stratification and coccolithophore blooms. Here we used hydrographic data to examine spatial relationships between stratification, nutrient concentrations, and the blooms. The cruise data were not synoptic; the data shown (Figures 6–8) were collected in late August through September of each year. Thus, it must be recognized that some of the spatial variability exhibited in these data may actually be temporal variability due to seasonal stratification breakdown associated with fall storms.

#### 3.2.1. Water Column

Figure 6 shows example profiles from stations within the bloom compared with stations outside of the bloom. While there is spatial variability throughout the survey, the selected stations and the differences between bloom and nonbloom profiles are generally representative. During bloom conditions in all 3 years (2009, 2011, and 2014), coccolithophores appeared to be in higher concentration above the pycnocline, based on fluorometer (high Chl  $a$ ) and transmissometer (low percent light transmission) data (Figure 6). In 2014, for example, only 20% of the light reached the detector across a 0.25-m path length (80% was lost). Outside of the bloom, Chl  $a$  was generally lower with maxima in the surface or subsurface (not shown), and percent light transmission was higher. Differences between bloom and nonbloom waters were often

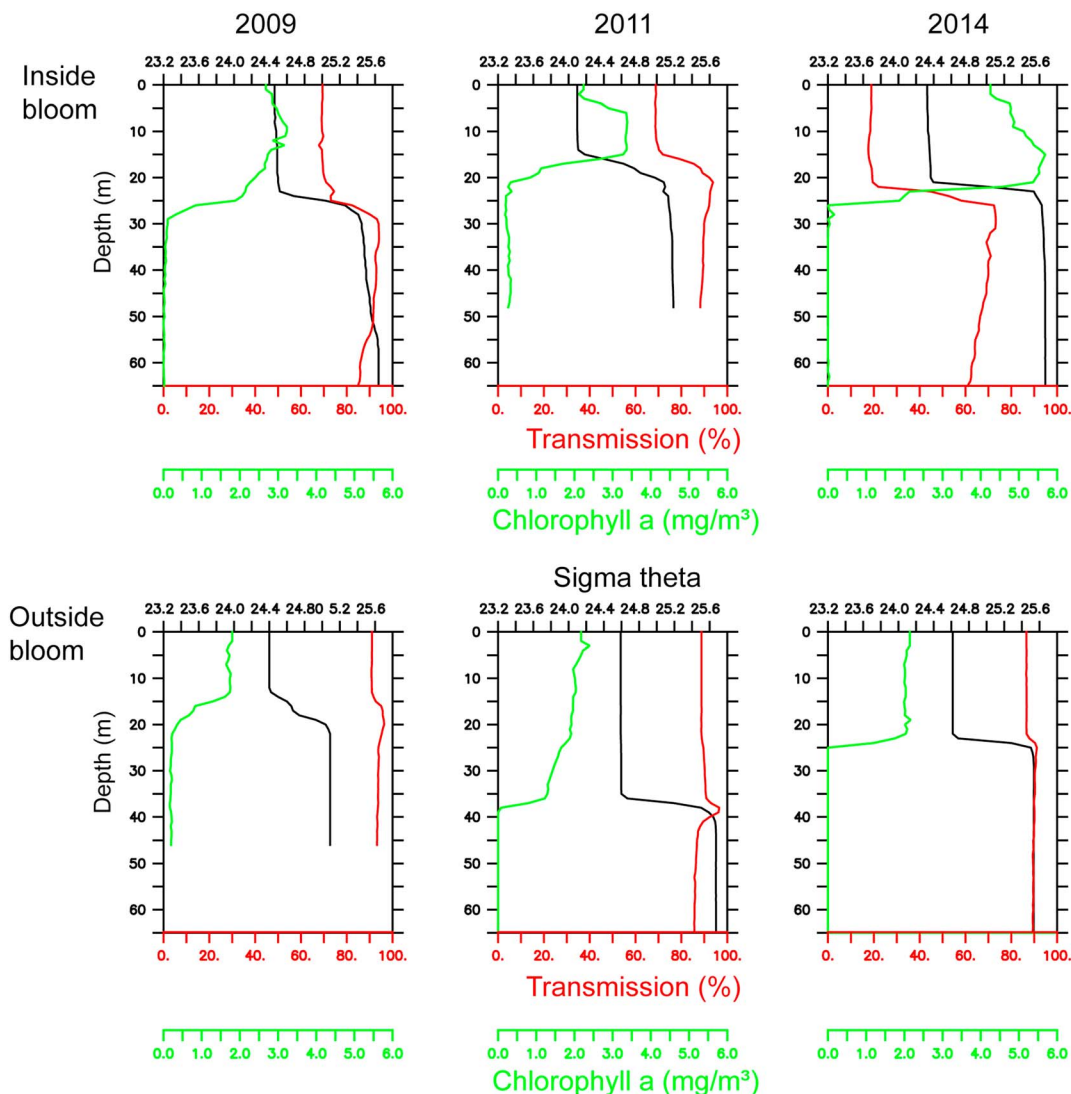


**Figure 6.** Bloom (top row) and nonbloom (bottom row) example profiles from 2009 (left column), 2011 (middle column), and 2014 (right column) for in situ calibrated fluorometer (Chlorophyll  $a$ : green), transmissometer (% light transmission: red), and density ( $\sigma_\theta$ : black). Cast locations shown in Figure 7.

mean over all 2009 stations. The magnitude of the measured stratification was comparable between the 70-m isobath transect and the gridded BASIS stations even though the southern inner and middle shelf of the BASIS grid was occupied a couple weeks prior to the 70-m isobath transect, demonstrating that the stratification variability observed in Figure 7 is primarily due to spatial variability. Stratification was lower both inshore and offshore of the bloom.

In 2011, differences in sampling timing between the southern 70-m isobath stations and the BASIS grid stations do account for differences in the stratification observed. In the southern middle shelf region, stratification was much lower as sampled by the 70-m isobath in late September than it was a couple weeks earlier when sampled by the BASIS survey, suggesting that a fall storm had mixed the water column in late September between the two surveys. In 2011, the coccolithophore bloom appears to align with the lower stratification waters of the inner shelf. This is particularly apparent in the region between 60° and 63°N (outside of the CBI region) where a strong cross-shelf gradient in stratification was evident in the BASIS survey. This gradient was not due to differences in sample timing. Even on the southern shelf (south of 59°N) the strongest bloom signal was associated with weaker stratification of the inner shelf.

In 2014, strong stratification was observed in both the middle and the outer shelves. A lack of data from the southern inner shelf inhibits comparison with the other years in this region. The innermost stations

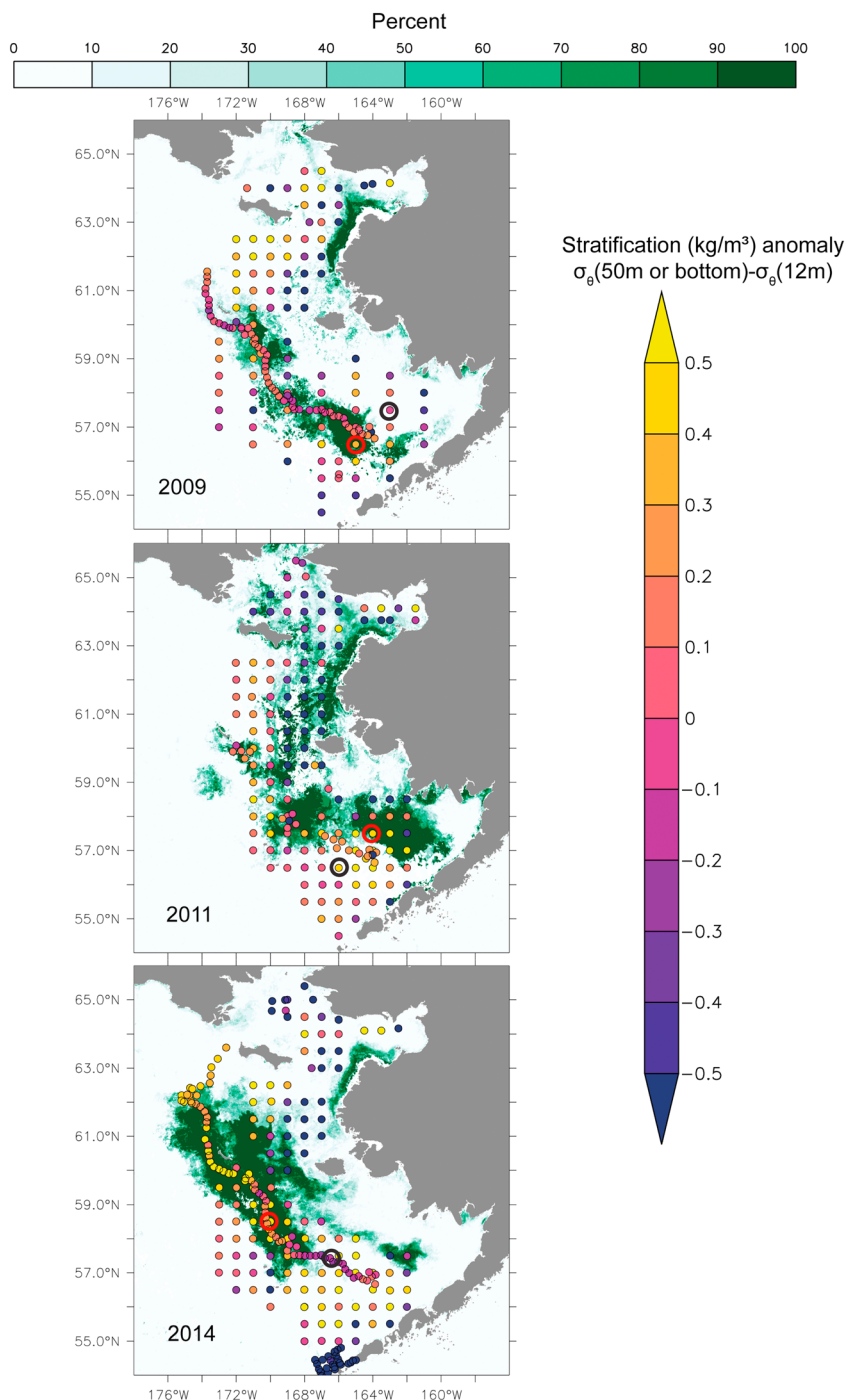


**Figure 7.** Stratification ( $\sigma_\theta$  [deeper of 50 m or bottom] –  $\sigma_\theta(12\text{ m})$ ;  $\text{kg/m}^3$ ; dots, color bar at the right) during August/September cruises overlaid on spatial CBI (percent; color bar at the top). Stratification is represented as anomaly from the mean of all stations for that year (2009 mean =  $0.74\text{ kg/m}^3$ ; 2011 mean =  $0.65\text{ kg/m}^3$ ; and 2014 mean =  $1.11\text{ kg/m}^3$ ). Location of casts shown in Figure 6 is denoted by circles (black: nonbloom; red: bloom). CBI = Coccolithophore Bloom Index.

along 57–57.5°N BASIS grid lines had low stratification associated with a small disconnected section of the bloom that appears related to the location of the inner front. The southeastern portion of the BASIS survey (mostly outside of the bloom except for those innermost stations) was occupied in August, while the 70-m isobath transect was occupied in late September accounting for the reduction of stratification in the

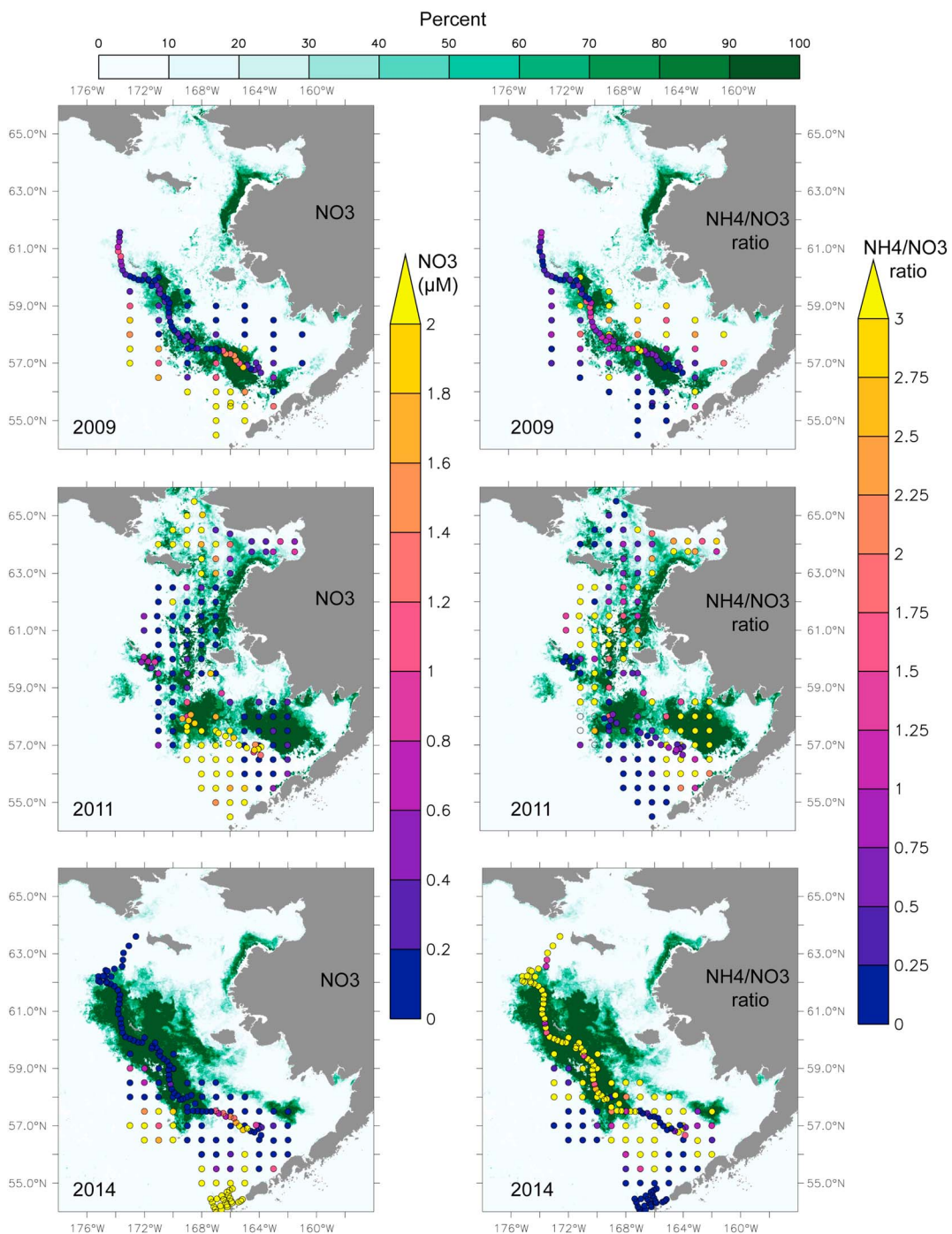


**Figure 8.** (left column) Nitrate ( $\mu\text{M}$ ) and (right column) ammonium:nitrate ratio (dots; color bars to the right of plots) in the surface mixed layer overlaid on spatial CBI (percent; color bar at the top). CBI = Coccolithophore Bloom Index.

southern part of the 70-m isobath transect as compared to the BASIS stations. Along the 70-m isobath transect, a gradient in stratification (weaker in the south) was coincident with the edge of the bloom.

Taken together, Figure 7 suggests that the coccolithophore blooms in 2009 and 2014 were associated with strong stratification in the middle shelf, while the bloom in 2011 was associated with weaker stratification on the inner shelf.

### 3.2.3. Nutrients

As noted previously, nutrient supply is important to the seasonal dynamics of phytoplankton succession (Margalef, 1978) and coccolithophores are superior competitors under nutrient limitation (Cermeno et al., 2008; Falkowski & Oliver, 2007; Iglesias-Rodriguez et al., 2002; Margalef, 1997). Oceanographic sampling has historically focused on nitrate, nitrite, phosphate, and silicate, but nitrate is not the sole source of nitrogen and *E. huxleyi* prefers ammonium to nitrate (Page et al., 1999; Song & Ward, 2007). In the upper 20 m of the middle shelf between 2003 and 2016, the mean concentration of ammonium was  $0.7 \pm 0.02 \mu\text{M}$  (SE,  $N = 4378$ ) with a maximum concentration of  $9.3 \mu\text{M}$ . The ratio of ammonium to nitrate may serve as an indicator of nutrient conditions favorable for coccolithophores (e.g., lower nitrate and higher ammonium).

In all 3 years, nitrate in the upper water column was at very low levels over much of the inner and middle shelf and the highest nitrate concentrations were measured on the outer shelf (Figure 8). In 2009, the highest ammonium:nitrate ratios were observed in nonbloom waters of the inner shelf. Values were very low at the southern and northern ends of the 70-m isobath transect but somewhat elevated between  $\sim 57$  and  $59^\circ\text{N}$ . The most concentrated part of the bloom (middle shelf south of  $58^\circ\text{N}$ ) was coincident with elevated nitrate and low ammonium:nitrate ratio.

In 2011, the southeasternmost part of the bloom on the inner shelf was coincident with low nitrate ( $< 0.2 \mu\text{M}$ ) and high ammonium:nitrate ratio ( $> 3$ ). The southern middle shelf (nonbloom region) had higher nitrate values than the bloom regions. Between  $\sim 58^\circ\text{N}$  and  $63^\circ\text{N}$ , nitrate was low and ammonium:nitrate ratio was high across most of the shelf. The 70-m isobath transect shows high nitrate and low ammonium:nitrate ratio at approximately the same locations ( $165\text{--}164^\circ\text{W}$ ) where the BASIS grid shows elevated ammonium:nitrate ratio. This observation is consistent with the previous analysis of stratification (Figure 7) suggesting that a fall storm had mixed the water column, bringing nitrate toward the surface, between the two surveys.

In 2014, higher nitrate values were observed only at the very edges of the bloom and entirely outside the bloom. Along the 70-m isobath transect, a gradient in nitrate and the ammonium:nitrate ratio was observed at the southern edge of the main bloom concentration. High ammonium:nitrate ratios were observed throughout the bloom region.

## 4. Discussion and Conclusions

Coccolithophore blooms have important biogeochemical implications including influencing the carbon cycle (e.g., Holligan et al., 1993; Milliman, 1993; Raitsos et al., 2006; Westbroek et al., 1993). Essentially, for every mole of calcium carbonate that coccolithophores produce, they consume 2 mol of bicarbonate and produce 1 mol of  $\text{CO}_2$ , thus affecting the biological carbon pump and the carbon cycle. The Bering Sea can be either a source or a sink of atmospheric  $\text{CO}_2$ , with the magnitude of coccolithophore blooms and the associated calcification playing a role (Iida et al., 2012). In addition, variability in the phytoplankton community structure and functional group dominance (e.g., diatoms vs. coccolithophores) is likely to influence trophic connections with the smaller coccolithophores resulting in longer and less efficient trophic chains. For example, it has been argued that coccolithophores may be a less desirable food source for microzooplankton in this region based on studies measuring growth and grazing for the  $<10\text{-}\mu\text{m}$  chlorophyll *a* size fraction (Olson & Strom, 2002), although new research measuring changes in coccolithophore cell counts has shown high mortality of coccolithophores by microzooplankton grazing ( $>60\%$  of daily growth) in the Celtic Sea (Mayers et al., 2018). The community composition of the microzooplankton may contribute to variations in grazing mortality as discussed by Mayers et al. (2018). As noted previously, the striking milky aquamarine color of the water during a coccolithophore bloom may also reduce foraging success for visual predators (Lovvorn et al., 2001).

Because of the important biogeochemical and ecosystem implications of coccolithophore blooms, their timely monitoring and reporting is necessary for ecosystem management. Over 20 years of satellite ocean color data have been used to characterize September coccolithophore blooms in the eastern Bering Sea spatially and temporally. An annual CBI, originally published in the 2016 Eastern Bering Sea Ecosystem Considerations report (Ladd et al., 2016), is intended to be updated annually and included in future iterations of the report for use by ecosystem management stakeholders.

This manuscript reports on a comparison of the CBI with in situ data from the region to the extent possible with limited and variable data coverage. Mooring M2 in the southeast Bering Sea has been

monitoring conditions on the middle shelf since 1995 comprising the longest, most consistent time series of ocean conditions in the region. Using these data to examine the relationship between summer stratification and the CBI, a significant nonlinear relationship was found. The CBI was higher during years with either very low or very high stratification. The CBI represents the eastern Bering Sea shelf south of 60°N, while the M2 mooring represents a single station in the middle shelf. Obviously, better spatial coverage in the assessment of stratification on the shelf would be very useful in this analysis but the time series do not exist. Thus, the relationship between CBI and M2 stratification should be treated with caution.

While strong stratification favors coccolithophore blooms in the middle domain and weak stratification favors blooms in the inner domain (Figure 5), it is likely that similar influences are responsible for coccolithophore blooms in the middle and the inner domains. Throughout summer (after the spring bloom depletes surface nutrients), the deep nutrient reservoir of the middle shelf provides the source of nutrients to the surface layer. On the middle shelf, the deep nutrient reservoir is accessed via episodic mixing. On the inner shelf, mixing at the inner front separating the middle from the inner domain provides access to the deep nutrient reservoir of the middle shelf (Kachel et al., 2002; Mordy et al., 2017). One hypothesis is that at very low stratification, the nutrients in the deeper layer are continuously mixed into the surface layer where they are quickly utilized by phytoplankton, resulting in low nutrients throughout the water column by the end of summer. At high stratification, more energy (i.e., wind mixing) is required for the surface mixed layer to access the deep nutrient reservoir. For example, in 2004, strong stratification of the water column led to poor nutrient supply to the euphotic zone causing a decline in phytoplankton production as well as reduced zooplankton grazing (Coyle et al., 2008; Strom & Fredrickson, 2008). Thus, at both very high and very low stratification, the system becomes strongly nutrient limited, a condition where coccolithophores out-compete other phytoplankton. At the midrange of stratification, higher levels of nutrients remain in the deep reservoir and can more easily be episodically injected into the surface mixed layer via wind-mixing events, allowing other phytoplankton to out-compete coccolithophores.

While we found no significant relationship between stratification and nutrients in the deep layer ( $> 30$  m) on interannual timescales to support this hypothesis, we note that nutrient data over the middle shelf in late summer for this analysis are limited and likely to be influenced by sample timing in relation to episodic mixing events, etc. Nutrient concentrations in the deep layer at the end of summer are a balance of all of the various sources (remineralization and advection) and sinks (productivity and vertical mixing), which are not resolved by our simple analysis.

Of the 3 years where we examined spatial correspondence between blooms and nutrient availability, all 3 years exhibited lower than average nitrate in the mixed layer in the bloom region. High ammonium:nitrate ratios corresponded with bloom presence in 2011 and 2014. In contrast, high ammonium:nitrate ratios were not associated with bloom presence in 2009, when other factors may have influenced phytoplankton dynamics. We cannot rule out the possibility that lower nitrate and higher ammonium were a product of the coccolithophore bloom (through nitrate drawdown and ammonification due to turnover of organic matter in bloom waters). However, there is some evidence suggesting that *E. huxleyi* may be better adapted to utilizing ammonium instead of nitrate compared with other phytoplankton species (Iwamoto & Shiraiwa, 2003), and genome sequencing of the *E. huxleyi* strain Culture Collection of Marine Phytoplankton 1516 revealed 24 predicted ammonium transporter genes but only 8 predicted nitrate transporter genes (Lefebvre et al., 2012; Read et al., 2013). Also, like red algae, *E. huxleyi* possesses NADH-specific (nicotinamide adenine dinucleotide) nitrate reductase, and the half-saturation constant ( $K_M$ ) of nitrate reductase in *E. huxleyi* for NADH was found to be high (23–80  $\mu$ M), compared to the lower  $K_M$  for NADH (3–5  $\mu$ M) found in higher plants and diatoms (Iwamoto & Shiraiwa, 2003), indicating poor affinity for nitrate.

*E. huxleyi* lacks photoinhibition and thus has tolerance for high light intensity (Nanninga & Tyrrell, 1996). However, in the eastern Bering Sea, we found no evidence that the light environment influenced the interannual variability of coccolithophore blooms. However, it is possible that the light environment influences coccolithophores on smaller spatial and temporal scales than resolved by this study.

Merico et al. (2004) suggest that the unusual conditions of 1997 allowed a seed population of coccolithophores in the Bering Sea that resulted in blooms in subsequent years (1998–2000), gradually fading away after the climate returned to less anomalous conditions. However, the subsequent high interannual

variability (particularly the alternating high/low coccolithophore bloom years from 2007 to 2012) suggests that interannual memory likely does not explain the high blooms in the late 1990s.

For comparison, the size of the largest bloom on the eastern Bering Sea shelf (omitting the region north of 60°N) in September 1997 was 166,000 km<sup>2</sup>, while a reported bloom in the North Atlantic in June 1998 was over 995,000 km<sup>2</sup> (Raittos et al., 2006); admittedly different algorithms were used to define the two blooms. While the Bering Sea blooms cover a small region in comparison to the North Atlantic, they can cover a substantial proportion of the eastern Bering Sea shelf. This implies that during extensive bloom years, there may be very little refuge available for shelf species that are negatively impacted by the bloom.

Maximum stratification on the Bering Sea shelf occurs in August (Ladd & Stabeno, 2012), which may help explain why coccolithophore blooms typically peak in September in this region (Iida et al., 2012). In the North Atlantic, coccolithophore blooms peak in June in association with high solar radiation and strong stratification (Raittos et al., 2006). In addition, Ladd and Stabeno (2012) found a negative correlation between the strength of August stratification and September chlorophyll *a* from satellite, further supporting the suggestion that stratification influences coccolithophore blooms.

While we have examined environmental influence on coccolithophore bloom formation, clearly, biological influences likely play a role. Olson and Strom (2002) found that reductions in microzooplankton grazing pressure on coccolithophores can allow the formation and temporal persistence of coccolithophore blooms in the Bering Sea. Thus, the top-down effects may also be important but are beyond the scope of this manuscript. Note that low-bloom years occurred during the full spectrum of August stratification conditions suggesting that while stratification extremes may be important to bloom formation, variables other than stratification are likely involved in suppressing blooms. Specifically, the alternating year bloom pattern observed since 2007 might be suggestive of a biological control, perhaps arising during blooms that might persist to reduce bloom formation in the succeeding year. For example, viruses are known to play a role in the demise of *E. huxleyi* blooms (Highfield et al., 2014; Lehahn et al., 2014; Martinez et al., 2012; Vardi et al., 2012). Also, a decoupling in phenology caused by population densities, dormancy, reproduction, and migration can also result in trophic mismatches (Durant et al., 2007; Edwards & Richardson, 2004).

We recognize that the monthly timescales used in this paper (August monthly average stratification and September monthly average CBI) are coarse. However, limitations to satellite data due to cloud cover in the region necessitate using a monthly average for the CBI. Stratification typically begins to breakdown in September with autumn storms, but the timing of stratification breakdown is highly variable. From limited cloud-free data, it appears that blooms often begin early in the month of September so stratification averaged over September would not represent interannual variability in initial conditions setting up the bloom. Note that September stratification does not significantly correlate with the CBI.

We have seen tantalizing evidence of environmental influence on the extent of coccolithophore blooms in the eastern Bering Sea, including a nonlinear relationship with stratification and possible relationships with nutrient availability (nitrate and ammonium). However, our tentative conclusions are restricted by temporal and spatial limitations to our historical data. To make headway on the causes and consequences of coccolithophore blooms in the eastern Bering Sea, the region needs to be consistently sampled with adequate spatial coverage both within and outside of the blooms and over an extended seasonal time frame to evaluate factors initiating bloom formation. In addition, process studies of nutrient uptake, phytoplankton competition, and succession in the region would also be extremely valuable.

## References

- Antia, N. J., Harrison, P. J., & Oliveira, L. (1991). The role of dissolved organic nitrogen in phytoplankton nutrition, cell biology and ecology. *Phycologia*, 30(1), 1–89. <https://doi.org/10.2216/I0031-8884-30-1-1.1>
- Baduini, C. L., Hyrenbach, K. D., Coyle, K. O., Pinchuk, A. I., Mendenhall, V., & Hunt, G. L. Jr. (2001). Mass mortality of short-tailed shearwaters in the south-eastern Bering Sea during summer 1997. *Fisheries Oceanography*, 10(1), 117–130. <https://doi.org/10.1046/j.1365-2419.2001.00156.x>
- Broerse, A. T. C., Tyrrell, T., Young, J. R., Poulton, A. J., Merico, A., Balch, W. M., & Miller, P. I. (2003). The cause of bright waters in the Bering Sea in winter. *Continental Shelf Research*, 23(16), 1579–1596. <https://doi.org/10.1016/j.csr.2003.07.001>
- Brown, C. W. (1995). Classification of coccolithophore blooms in ocean color imagery. Greenbelt, MD. Retrieved from <https://ntrs.nasa.gov/archive/nasa/casi.ntrs.nasa.gov/19950025429.pdf>
- Brown, C. W., & Yoder, J. A. (1994). Coccolithophorid blooms in the global ocean. *Journal of Geophysical Research*, 99(C4), 7467–7482. <https://doi.org/10.1029/93JC02156>

- Cermeno, P., Dutkiewicz, S., Harris, R. P., Follows, M., Schofield, O., & Falkowski, P. G. (2008). The role of nutricline depth in regulating the ocean carbon cycle. *Proceedings of the National Academy of Sciences of the United States of America*, 105(51), 20,344–20,349. <https://doi.org/10.1073/pnas.0811302106>
- Coachman, L. K., & Charnell, R. L. (1979). On lateral water mass interaction—A case study, Bristol Bay, Alaska. *Journal of Physical Oceanography*, 9(2), 278–297. [https://doi.org/10.1175/1520-0485\(1979\)009<0278:OLWMIC>2.0.CO;2](https://doi.org/10.1175/1520-0485(1979)009<0278:OLWMIC>2.0.CO;2)
- Coyle, K. O., Pinchuk, A. I., Eisner, L. B., & Napp, J. M. (2008). Zooplankton species composition, abundance and biomass on the eastern Bering Sea shelf during summer: The potential role of water-column stability and nutrients in structuring the zooplankton community. *Deep-Sea Research Part II*, 55(16–17), 1775–1791. <https://doi.org/10.1016/j.dsr2.2008.04.029>
- Delille, B., Harlay, J., Zondervan, I., Jacquet, S., Chou, L., Wollast, R., et al. (2005). Response of primary production and calcification to changes of pCO<sub>2</sub> during experimental blooms of the coccolithophorid *Emiliania huxleyi*. *Global Biogeochemical Cycles*, 19, GB2023. <https://doi.org/10.1029/2004GB002318>
- Durant, J. M., Hjermann, D. Ø., Ottersen, G., & Stenseth, N. C. (2007). Climate and the match or mismatch between predator requirements and resource availability. *Climate Research*, 33(3), 271–283. <https://doi.org/10.3354/cr033271>
- Edwards, M., & Richardson, A. J. (2004). Impact of climate change on marine pelagic phenology and trophic mismatch. *Nature*, 430(7002), 881–884. <https://doi.org/10.1038/nature02808>
- Eisner, L. B., Gann, J. C., Ladd, C., Cieciel, K. D., & Mordy, C. W. (2016). Late summer/early fall phytoplankton biomass (chlorophyll *a*) in the eastern Bering Sea: Spatial and temporal variations and factors affecting chlorophyll *a* concentrations. *Deep Sea Research, Part II*, 134, 100–114. <https://doi.org/10.1016/j.dsr2.2015.07.012>
- Falkowski, P. G., & Oliver, M. J. (2007). Mix and match: How climate selects phytoplankton. *Nature Reviews Microbiology*, 5, 813. <https://doi.org/10.1038/nrmicro1751>
- Favorite, F., Dodimead, A. J., & Nasu, K. (1976). Oceanography of the subarctic Pacific region, 1960–71. *International North Pacific Fisheries Commission, Bulletin*, 33, 187.
- Gordon, L. I., Jennings Jr., J. C., Ross, A. A., & Krest, J. M. (1994). A suggested protocol for continuous flow automated analysis of seawater nutrients (phosphate, nitrate, nitrite, and silicic acid) in the WOCE hydrographic program and the joint global ocean fluxes study. In *WHP Office Report WHP 91-1, Part 3.1.3: WHP Operations and Methods, WOCE Report No. 68/91* (pp. 52). Woods Hole, MA: WOCE Hydrographic Program Office. Retrieved from [http://whpo.ucsd.edu/manuals/pdf/91\\_1/gordnut.pdf](http://whpo.ucsd.edu/manuals/pdf/91_1/gordnut.pdf)
- Harada, N., Sato, M., Oguri, K., Hagino, K., Okazaki, Y., Katsuki, K., et al. (2012). Enhancement of coccolithophorid blooms in the Bering Sea by recent environmental changes. *Global Biogeochemical Cycles*, 26, GB2036. <https://doi.org/10.1029/2011GB004177>
- Haynie, A. C., & Huntington, H. P. (2016). Strong connections, loose coupling: The influence of the Bering Sea ecosystem on commercial fisheries and subsistence harvests in Alaska. *Ecology and Society*, 21(4), 6. <https://doi.org/10.5751/ES-08729-210406>
- Highfield, A., Evans, C., Walne, A., Miller, P. I., & Schroeder, D. C. (2014). How many coccolithovirus genotypes does it take to terminate an *Emiliania huxleyi* bloom? *Virology*, 466, 138–145. <https://doi.org/10.1016/j.virol.2014.07.017>
- Holligan, P. M., Fernández, E., Aiken, J., Balch, W. M., Boyd, P., Burkhill, P. H., et al. (1993). A biogeochemical study of the coccolithophore, *Emiliania huxleyi*, in the North Atlantic. *Global Biogeochemical Cycles*, 7(4), 879–900. <https://doi.org/10.1029/93GB01731>
- Hopkins, J., Henson, S. A., Painter, S. C., Tyrrell, T., & Poulton, A. J. (2015). Phenological characteristics of global coccolithophore blooms. *Global Biogeochemical Cycles*, 29, 239–253. <https://doi.org/10.1002/2014GB004919>
- Houdan, A., Probert, I., Van Lenning, K., & Lefebvre, S. (2005). Comparison of photosynthetic responses in diploid and haploid life-cycle phases of *Emiliania huxleyi* (Prymnesiophyceae). *Marine Ecology-Progress Series*, 292, 139–146. <https://doi.org/10.3354/meps292139>
- Hunt, G. L., Baduini, C. L., Brodeur, R. D., Coyle, K. O., Kachel, N. B., Napp, J. M., et al. (1999). The Bering Sea in 1998: The second consecutive year of extreme weather-forced anomalies. *Eos, Transactions American Geophysical Union*, 80(47), 561–566. <https://doi.org/10.1029/EO080i047p00561>
- Iglesias-Rodriguez, M. D., Brown, C. W., Doney, S. C., Kleypas, J., Kolber, D., Kolber, Z., et al. (2002). Representing key phytoplankton functional groups in ocean carbon cycle models: Coccolithophorids. *Global Biogeochemical Cycles*, 16(4), 1100. <https://doi.org/10.1029/2001GB001454>
- Iglesias-Rodriguez, M. D., Halloran, P. R., Rickaby, R. E. M., Hall, I. R., Colmenero-Hidalgo, E., Gittins, J. R., et al. (2008). Phytoplankton calcification in a high-CO<sub>2</sub> world. *Science*, 320(5874), 336–340. <https://doi.org/10.1126/science.1154122>
- Iida, T., Mizobata, K., & Saitoh, S. I. (2012). Interannual variability of coccolithophore *Emiliania huxleyi* blooms in response to changes in water column stability in the eastern Bering Sea. *Continental Shelf Research*, 34, 7–17. <https://doi.org/10.1016/j.csr.2011.11.007>
- Iida, T., Saitoh, S. I., Miyamura, T., Toratani, M., Fukushima, H., & Shiga, N. (2002). Temporal and spatial variability of coccolithophore blooms in the eastern Bering Sea, 1998–2001. *Progress in Oceanography*, 55(1–2), 165–175. [https://doi.org/10.1016/S0079-6611\(02\)00076-9](https://doi.org/10.1016/S0079-6611(02)00076-9)
- Irigoién, X., Flynn, K. J., & Harris, R. P. (2005). Phytoplankton blooms: A 'loophole' in microzooplankton grazing impact? *Journal of Plankton Research*, 27(4), 313–321. <https://doi.org/10.1093/plankt/fbi011>
- Iwamoto, K., & Shiraiwa, Y. (2003). Characterization of NADH: Nitrate reductase from the coccolithophorid *Emiliania huxleyi* (Lohman) Hay & Mohler (Haptophyceae). *Marine Biotechnology*, 5(1), 20–26. <https://doi.org/10.1007/s10126-002-0051-8>
- Joint Global Ocean Flux Study (1994). Protocols for the Joint Global Ocean Flux Study (JGOFS) core measurements. Paris, France.
- Kachel, N. B., Hunt, G. L. Jr., Salo, S. A., Schumacher, J. D., Stabeno, P. J., & Whittlestone, T. E. (2002). Characteristics and variability of the inner front of the southeastern Bering Sea. *Deep Sea Research Part II*, 49(26), 5889–5909. [https://doi.org/10.1016/S0967-0645\(02\)00324-7](https://doi.org/10.1016/S0967-0645(02)00324-7)
- Kalnay, E., Kanamitsu, M., Kistler, R., Collins, W., Deaven, D., Gandin, L., et al. (1996). The NCEP/NCAR 40-year reanalysis project. *Bulletin of the American Meteorological Society*, 77(3), 437–471. [https://doi.org/10.1175/1520-0477\(1996\)077<0437:TNYRP>2.0.CO;2](https://doi.org/10.1175/1520-0477(1996)077<0437:TNYRP>2.0.CO;2)
- Kinder, T. H., & Coachman, L. K. (1978). The front overlaying the continental slope in the eastern Bering Sea. *Journal of Geophysical Research*, 83, 4551–4559. <https://doi.org/10.1029/JC083iC09p04551>
- Kinder, T. H., & Schumacher, J. D. (1981). Hydrographic structure over the continental shelf of the southeast Bering Sea. In D. W. Hood, & J. A. Calder (Eds.), *The Eastern Bering Sea Shelf: Oceanography and Resources* (Vol. 1, pp. 31–52). Seattle, WA: University of Washington Press.
- Ladd, C., Salo, S., & Eisner, L. (2016). Coccolithophores in the Bering Sea. In S. Zador (Ed.), *Ecosystem considerations 2016, stock assessment and fishery evaluation report* (pp. 87–90). Anchorage, AK: North Pacific fisheries management council. Retrieved from <https://www.afsc.noaa.gov/REFM/Docs/2016/ecosysEBS.pdf>
- Ladd, C., & Stabeno, P. J. (2012). Stratification on the eastern Bering Sea shelf revisited. *Deep Sea Research, Part II*, 65–70, 72–83. <https://doi.org/10.1016/j.dsr2.2012.02.009>
- Lefebvre, S. C., Benner, I., Stillman, J. H., Parker, A. E., Drake, M. K., Rossignol, P. E., et al. (2012). Nitrogen source and pCO<sub>2</sub> synergistically affect carbon allocation, growth and morphology of the coccolithophore *Emiliania huxleyi*: Potential implications of ocean acidification for the carbon cycle. *Global Change Biology*, 18(2), 493–503. <https://doi.org/10.1111/j.1365-2486.2011.02575.x>

- Lehahn, Y., Koren, I., Schatz, D., Frada, M., Sheyn, U., Boss, E., et al. (2014). Decoupling physical from biological processes to assess the impact of viruses on a mesoscale algal bloom. *Current Biology*, 24(17), 2041–2046. <https://doi.org/10.1016/j.cub.2014.07.046>
- Lovvorn, J. R., Baduini, C. L., & Hunt, G. L. (2001). Modeling underwater visual and filter feeding by planktivorous shearwaters in unusual sea conditions. *Ecology*, 82(8), 2342–2356. [https://doi.org/10.1890/0012-9658\(2001\)082\[2342:MUVAFF\]2.0.CO;2](https://doi.org/10.1890/0012-9658(2001)082[2342:MUVAFF]2.0.CO;2)
- Margalef, R. (1978). Life-forms of phytoplankton as survival alternatives in an unstable environment. *Oceanologica Acta*, 1(4), 493–509.
- Margalef, R. (1997). Turbulence and marine life. *Scientia Marina*, 61, 109–123.
- Martinez, J. M., Schroeder, D. C., & Wilson, W. H. (2012). Dynamics and genotypic composition of *Emiliania huxleyi* and their co-occurring viruses during a coccolithophore bloom in the North Sea. *FEMS Microbiology Ecology*, 81(2), 315–323. <https://doi.org/10.1111/j.1574-6941.2012.01349.x>
- Mayers, K. M. J., Poultney, A. J., Daniels, C. J., Wells, S. R., Woodward, E. M. S., Tarran, G. A., et al. (2018). Growth and mortality of coccolithophores during spring in a temperate Shelf Sea (Celtic Sea, April 2015). *Progress in Oceanography*. <https://doi.org/10.1016/j.pocean.2018.02.024>
- Merico, A., Tyrrell, T., Brown, C. W., Groom, S. B., & Miller, P. I. (2003). Analysis of satellite imagery for *Emiliania huxleyi* blooms in the Bering Sea before 1997. *Geophysical Research Letters*, 30(6), 1337. <https://doi.org/10.1029/2002GL016648>
- Merico, A., Tyrrell, T., Lessard, E. J., Oguz, T., Stabeno, P. J., Zeeman, S. I., & Whittlestone, T. E. (2004). Modelling phytoplankton succession on the Bering Sea shelf: Role of climate influences and trophic interactions in generating *Emiliania huxleyi* blooms 1997–2000. *Deep Sea Research Part I: Oceanographic Research Papers*, 51(12), 1803–1826. <https://doi.org/10.1016/j.dsr.2004.07.003>
- Milliman, J. D. (1993). Production and accumulation of calcium-carbonate in the ocean—Budget of a nonsteady state. *Global Biogeochemical Cycles*, 7(4), 927–957. <https://doi.org/10.1029/93GB02524>
- Mordy, C. W., Devol, A., Eisner, L. B., Kachel, N., Ladd, C., Lomas, M. W., et al. (2017). Nutrient and phytoplankton dynamics on the inner shelf of the eastern Bering Sea. *Journal of Geophysical Research: Oceans*, 122, 2422–2440. <https://doi.org/10.1002/2016JC012071>
- Nanninga, H. J., & Tyrrell, T. (1996). Importance of light for the formation of algal blooms by *Emiliania huxleyi*. *Marine Ecology Progress Series*, 136(1–3), 195–203. <https://doi.org/10.3354/meps136195>
- Napp, J. M., & Hunt, G. L. Jr. (2001). Anomalous conditions in the south-eastern Bering Sea 1997: Linkages among climate, weather, ocean, and biology. *Fisheries Oceanography*, 10(1), 61–68. <https://doi.org/10.1046/j.1365-2419.2001.00155.x>
- NASA Goddard Space Flight Center, Ocean Ecology Laboratory, Ocean Biology Processing Group (2014a Reprocessing-a). Moderate-resolution Imaging Spectroradiometer (MODIS) Aqua ocean color data. Retrieved from <http://oceancolor.gsfc.nasa.gov>
- NASA Goddard Space Flight Center, Ocean Ecology Laboratory, Ocean Biology Processing Group (2014b Reprocessing-b). Sea-viewing Wide Field-of-view Sensor (SeaWiFS) ocean color data. Retrieved from <http://oceancolor.gsfc.nasa.gov>
- Olson, M. B., & Strom, S. L. (2002). Phytoplankton growth, microzooplankton herbivory and community structure in the southeast Bering Sea: Insight into the formation and temporal persistence of an *Emiliania huxleyi* bloom. *Deep Sea Research Part II*, 49(26), 5969–5990. [https://doi.org/10.1016/S0967-0645\(02\)00329-6](https://doi.org/10.1016/S0967-0645(02)00329-6)
- Page, S., Hipkin, C. R., & Flynn, K. J. (1999). Interactions between nitrate and ammonium in *Emiliania huxleyi*. *Journal of Experimental Marine Biology and Ecology*, 236(2), 307–319. [https://doi.org/10.1016/s0022-0981\(98\)00212-3](https://doi.org/10.1016/s0022-0981(98)00212-3)
- Parsons, T. R., Maita, Y., & Lalli, C. M. (1984). *A manual of chemical and biological methods for seawater analysis*. Oxford: Pergamon Press.
- Raitt, D. E., Lavender, S. J., Pradhan, Y., Tyrrell, T., Reid, P. C., & Edwards, M. (2006). Coccolithophore bloom size variation in response to the regional environment of the subarctic North Atlantic. *Limnology and Oceanography*, 51(5), 2122–2130. <https://doi.org/10.4319/lo.2006.51.5.2122>
- Read, B. A., Kegel, J., Klute, M. J., Kuo, A., Lefebvre, S. C., Maumus, F., et al. (2013). Pan genome of the phytoplankton *Emiliania* underpins its global distribution. *Nature*, 499(7457), 209–213. <https://doi.org/10.1038/nature12221>
- Riebesell, U., Zondervan, I., Rost, B., Tortell, P. D., Zeebe, R. E., & Morel, F. M. M. (2000). Reduced calcification of marine plankton in response to increased atmospheric CO<sub>2</sub>. *Nature*, 407(6802), 364–367. <https://doi.org/10.1038/35030078>
- Riegman, R., Stolte, W., Noordeloos, A. A. M., & Slezak, D. (2000). Nutrient uptake and alkaline phosphatase (ec 3:1:3:1) activity of *Emiliania huxleyi* (PRYMNESIOPHYCEAE) during growth under N and P limitation in continuous cultures. *Journal of Phycology*, 36(1), 87–96. <https://doi.org/10.1046/j.1529-8817.2000.99023.x>
- Robinson, W. D. (2000). The updated SeaWiFS coccolithophore algorithm. Greenbelt, MD. Retrieved from <https://ntrs.nasa.gov/archive/nasa/casi.ntrs.nasa.gov/20010072019.pdf>
- Sambrotto, R. N., Niebauer, H. J., Goering, J. J., & Iverson, R. L. (1986). Relationships among vertical mixing, nitrate uptake, and phytoplankton growth during the spring bloom in the southeast Bering Sea middle shelf. *Continental Shelf Research*, 5(1–2), 161–198. [https://doi.org/10.1016/0278-4343\(86\)90014-2](https://doi.org/10.1016/0278-4343(86)90014-2)
- Sasaki, H., Saitoh, S., & Kishino, M. (2001). Bio-optical properties of seawater in the western Subarctic gyre and Alaskan gyre in the subarctic North Pacific and the southern Bering Sea during the summer of 1997. *Journal of Oceanography*, 57(3), 275–284. <https://doi.org/10.1023/A:1012478420867>
- Schumacher, J. D., & Stabeno, P. J. (1998). The continental shelf of the Bering Sea. In A. R. Robinson & K. H. Brink (Eds.), *The sea: The global coastal ocean: regional studies and synthesis* (Vol. 11, pp. 789–822). New York: John Wiley and Sons.
- Song, B., & Ward, B. B. (2007). Molecular cloning and characterization of high-affinity nitrate transporters in marine phytoplankton. *Journal of Phycology*, 43(3), 542–552. <https://doi.org/10.1111/j.1529-8817.2007.00352.x>
- Stabeno, P. J., Bond, N. A., Kachel, N. B., Salo, S. A., & Schumacher, J. D. (2001). On the temporal variability of the physical environment over the south-eastern Bering Sea. *Fisheries Oceanography*, 10(1), 81–98. <https://doi.org/10.1046/j.1365-2419.2001.00157.x>
- Stabeno, P. J., Duffy-Anderson, J. T., Eisner, L. B., Farley, E. V., Heintz, R. A., & Mordy, C. W. (2017). Return of warm conditions in the south-eastern Bering Sea: Physics to fluorescence. *PLoS One*, 12(9), e0185464. <https://doi.org/10.1371/journal.pone.0185464>
- Stabeno, P. J., Farley, E. V., Kachel, N., Moore, S. E., Mordy, C., Napp, J. M., et al. (2012). A comparison of the physics of the northern and southern shelves of the eastern Bering Sea and some implications for the ecosystem. *Deep Sea Research, Part II*, 65–70, 14–30. <https://doi.org/10.1016/j.dsr2.2012.02.019>
- Stabeno, P. J., Kachel, N. B., Moore, S. E., Napp, J. M., Sigler, M., Yamaguchi, A., & Zerbini, A. (2012). Comparison of warm and cold years on the southeastern Bering Sea shelf and some implications for the ecosystem. *Deep Sea Research, Part II*, 65–70, 31–45. <https://doi.org/10.1016/j.dsr2.2012.02.020>
- Stabeno, P. J., Napp, J. M., Mordy, C., & Whittlestone, T. E. (2010). Factors influencing physical structure and lower trophic levels of the eastern Bering Sea shelf in 2005: Sea ice, tides and winds. *Progress in Oceanography*, 85(3–4), 180–196. <https://doi.org/10.1016/j.pocean.2010.02.010>
- Stockwell, D. A., Whittlestone, T. E., Zeeman, S. I., Coyle, K. O., Napp, J. M., Brodeur, R. D., et al. (2001). Anomalous conditions in the south-eastern Bering Sea, 1997: Nutrients, phytoplankton and zooplankton. *Fisheries Oceanography*, 10(1), 99–116. <https://doi.org/10.1046/j.1365-2419.2001.00158.x>

- Strom, S. L., & Fredrickson, K. A. (2008). Intense stratification leads to phytoplankton nutrient limitation and reduced microzooplankton grazing in the southeastern Bering Sea. *Deep-Sea Research Part II*, 55(16–17), 1761–1774. <https://doi.org/10.1016/j.dsr2.2008.04.008>
- Tyrrell, T., & Taylor, A. H. (1996). A modelling study of *Emiliana huxleyi* in the NE Atlantic. *Journal of Marine Systems*, 9(1–2), 83–112. [https://doi.org/10.1016/0924-7963\(96\)00019-X](https://doi.org/10.1016/0924-7963(96)00019-X)
- Vance, T. C., Schumacher, J. D., Stabeno, P. J., Baier, C. T., Wyllie-Echeverria, T., Tynan, C. T., et al. (1998). Aquamarine waters recorded for first time in eastern Bering Sea. *Eos, Transactions American Geophysical Union*, 79(10), 121–126. <https://doi.org/10.1029/98EO00083>
- Vardi, A., Haramaty, L., Van Mooy, B. A. S., Fredricks, H. F., Kimmance, S. A., Larsen, A., & Bidle, K. D. (2012). Host-virus dynamics and subcellular controls of cell fate in a natural coccolithophore population. *Proceedings of the National Academy of Sciences of the United States of America*, 109(47), 19,327–19,332. <https://doi.org/10.1073/pnas.1208895109>
- Westbroek, P., Brown, C. W., Vanbleijswijk, J., Brownlee, C., Brummer, G. J., Conte, M., et al. (1993). A model system approach to biological climate forcing. The example of *Emiliana huxleyi*. *Global and Planetary Change*, 8(1–2), 27–46. [https://doi.org/10.1016/0921-8181\(93\)90061-r](https://doi.org/10.1016/0921-8181(93)90061-r)
- Whitledge, T. E., Reeburgh, W. S., & Walsh, J. J. (1986). Seasonal inorganic nitrogen distribution and dynamics in the southeastern Bering Sea. *Continental Shelf Research*, 5(1–2), 109–132. [https://doi.org/10.1016/0278-4343\(86\)90012-9](https://doi.org/10.1016/0278-4343(86)90012-9)
- Zondervan, I., Zeebe, R. E., Rost, B., & Riebesell, U. (2001). Decreasing marine biogenic calcification: A negative feedback on rising atmospheric pCO<sub>2</sub>. *Global Biogeochemical Cycles*, 15(2), 507–516. <https://doi.org/10.1029/2000GB001321>